



HAL
open science

Constraints from loess on the Hf–Nd isotopic composition of the upper continental crust

Catherine Chauvel, Marion Garçon, Sarah Bureau, Adeline Besnault,
Bor-Ming Jahn, Zhongli Ding

► **To cite this version:**

Catherine Chauvel, Marion Garçon, Sarah Bureau, Adeline Besnault, Bor-Ming Jahn, et al.. Constraints from loess on the Hf–Nd isotopic composition of the upper continental crust. *Earth and Planetary Science Letters*, 2014, 388, pp.48-58. 10.1016/j.epsl.2013.11.045 . hal-03758816

HAL Id: hal-03758816

<https://hal.science/hal-03758816v1>

Submitted on 23 Aug 2022

HAL is a multi-disciplinary open access archive for the deposit and dissemination of scientific research documents, whether they are published or not. The documents may come from teaching and research institutions in France or abroad, or from public or private research centers.

L'archive ouverte pluridisciplinaire **HAL**, est destinée au dépôt et à la diffusion de documents scientifiques de niveau recherche, publiés ou non, émanant des établissements d'enseignement et de recherche français ou étrangers, des laboratoires publics ou privés.

1
2
3
4
5
6
7
8
9
10
11
12
13
14
15
16
17
18
19
20
21
22
23
24

Constraints from loess on the Hf-Nd isotopic composition of the upper continental crust

Catherine Chauvel^{1,2}, Marion Garçon^{1,2}, Sarah Bureau^{1,2}, Adeline Besnault^{1,2*}, Bor-ming Jahn³ and Zhongli Ding^{4,5}

1: Univ. Grenoble Alpes, ISTERre, F-38041 Grenoble, France

2: CNRS, ISTERre, F-38041 Grenoble, France

3: Department of Geological Sciences, National Taiwan University, Taipei, 106 Taiwan

4: Key Laboratory of Cenozoic Geology and Environment, Institute of Geology and Geophysics, Chinese Academy of Sciences, Beituchengxi Road 19, Chaoyang District, Beijing 100029, China

5: Chinese Academy of Sciences, Sanlihe Road 52, Xicheng, Beijing 100864, China

*: Now at INRA Orléans 2163 avenue de la Pomme de Pin CS 40001 45075 Orléans Cedex 02, France

Corresponding author: Catherine Chauvel, e-mail: Catherine.chauvel@ujf-grenoble.fr, tel: +334 76 63 59 12, address: ISTERre, Campus Universitaire, BP 53, F-38041 Grenoble Cedex 09, France.

Keywords: Nd and Hf isotopes, upper continental crust, Sm/Nd and Lu/Hf ratios

25 **Abstract**

26 Knowledge of the average composition of the upper continental crust is crucial to
27 establish not only how it formed but also when. While well constrained averages
28 have been suggested for its major and trace element composition, no values exist
29 for its Nd and Hf isotopic compositions even though radiogenic isotopic systems
30 provide valuable information on its average model age.

31 Here we present Nd and Hf isotopic data determined on a large number of loess
32 deposits from several continents. We demonstrate that these deposits have very
33 uniform Nd and Hf isotopic compositions. We obtain an average Nd isotopic
34 composition that is similar to previous estimates for the upper continental crust
35 ($\epsilon_{Nd} = -10.3 \pm 1.2$ (1σ)) and we establish a new Hf average value at $\epsilon_{Hf} = -13.2 \pm 2$
36 (1σ). This average falls on the “Terrestrial Array”, demonstrating that the two
37 parent-daughter ratios are not decoupled during crust formation. Trace element
38 data acquired on the same set of samples allow us to calculate an average
39 $^{147}\text{Sm}/^{144}\text{Nd}$ ratio for the upper continental crust: 0.1193 ± 0.0026 , a value
40 slightly higher than previous estimates. Based on the relationship between
41 Sm/Nd and Nd isotopes, we estimate the average Nd extraction age of upper
42 continental crust from the depleted mantle at $T_{DM}(\text{Nd}) = 1.82 \pm 0.07$ Ga. This
43 model age is entirely consistent with previous suggestions made for example by
44 Goldstein et al. [1984].

45 Assuming that for each individual sample, the Hf model age cannot be younger
46 than the Nd model age, our new Nd-Hf isotopic data provide a value for the very
47 poorly known $^{176}\text{Lu}/^{177}\text{Hf}$ ratio of the upper crust. Our estimate is $^{176}\text{Lu}/^{177}\text{Hf} =$
48 0.0125 ± 0.0018 , a value significantly lower than commonly used values [0.0150 –
49 0.0159, *Griffin et al.*, 2002; *Goodge and Vervoort*, 2006; *Hawkesworth et al.*, 2010]
50 but higher than Rudnick and Gao’s [2003] estimate of 0.0083. The impact of our
51 new $^{176}\text{Lu}/^{177}\text{Hf}$ ratio on crustal model ages of zircon populations is not simple to
52 evaluate but the Hf model ages calculated with this new Lu/Hf ratio could be
53 younger by up to 500 Ma.

54

55

56

57

58

59 **1 - Introduction**

60 The formation of the continental crust was certainly one of the most important
61 events that affected the overall composition of the Earth, because the isolation at
62 the surface of a light and enriched layer left behind a depleted residue in the
63 mantle. This observation explains why so many studies concentrate on the
64 processes that produce continental crust and on the timing of crustal growth
65 [e.g., *Armstrong, 1968; McCulloch and Wasserburg, 1978; Armstrong, 1981;*
66 *Allègre and Rousseau, 1984; Goldstein et al., 1984; Taylor and McLennan, 1985;*
67 *Condie, 1993; Wedepohl, 1995; Gallet et al., 1998; Vervoort et al., 2000; Griffin et*
68 *al., 2002; Rudnick and Gao, 2003; Harrison et al., 2005; Hawkesworth and Kemp,*
69 *2006; Blichert-toft and Albarède, 2008; Belousova et al., 2010; Hawkesworth et al.,*
70 *2010; Kemp et al., 2010; Dhuime et al., 2011; Garçon et al., 2011; Iizuka et al.,*
71 *2013*]. In this study, we focus on the information provided by two isotopic
72 systems, Sm-Nd and Lu-Hf. The two systems are strongly coupled during
73 magmatic processes leading to the definition of the “Terrestrial array”, an array
74 along which all terrestrial magmas fall [*Vervoort et al., 1999; Vervoort et al.,*
75 *2011*]. However, even though crustal magmas fall on the “Terrestrial Array” the
76 location of the average composition of the continental crust remains unknown.

77 Knowing the position of present-day average crust on the Terrestrial array is
78 important because it provides information not only on the processes active
79 during the formation of the crust but also because the two isotopic systems
80 record the past history of crustal materials and can be used to calculate an
81 average extraction age of crust from the mantle. Finally, by using the constraints
82 provided by the Sm-Nd isotopic system and those coming from the Lu-Hf isotopic
83 system, we can evaluate the average crustal $^{176}\text{Lu}/^{177}\text{Hf}$ ratio, a very poorly
84 known but crucial parameter necessary to calculate crustal residence ages of
85 zircon populations [e.g., *Griffin et al., 2002; Harrison et al., 2005; Kemp et al.,*

86 2007; *Blichert-toft and Albarède, 2008; Belousova et al., 2010; Kemp et al., 2010;*
87 *Condie et al., 2011; Yao et al., 2011; Iizuka et al., 2013*].

88 To address all these issues, we focus on a combined Nd and Hf isotopic study of a
89 variety of recent loess deposits from several continents. Loess deposits result
90 from the local accumulation of windblown dust coming from usually large
91 continental areas. They represent natural mixtures of erosion products of
92 continental surfaces and were therefore used by several previous workers to
93 determine the average composition of the upper continental crust [e.g., *Taylor*
94 *and McLennan, 1981; Taylor et al., 1983; Taylor and McLennan, 1985, 1995;*
95 *Barth et al., 2000*]. We show that they are excellent proxies for the average
96 composition of large areas of upper continental crust for both the Sm-Nd and the
97 Lu-Hf isotopic systems. We then suggest an average value for the upper
98 continental crust for the two systems and we determine an average model age.
99 Finally, the combined Nd and Hf isotopic data allow us to suggest a value for the
100 $^{176}\text{Lu}/^{177}\text{Hf}$ ratio of the upper continental crust.

101

102 **2 - Source of samples**

103 The samples in this study were collected from several locations around the
104 world: Western Europe, Tajikistan, China and Argentina (see Figure 1). Most
105 were previously studied by Gallet and co-workers [*Gallet et al., 1996; Gallet et al.,*
106 *1998; Jahn et al., 2001*] who reported major and trace element data as well as Nd
107 and Sr isotopic compositions for loess samples from China, Western Europe and
108 Argentina. The Tajikistan loess deposits come from the Chashmanigar section
109 and were previously studied by Ding et al. [2002] and by Yang et al. [2006] who
110 used sedimentological and major element data to constrain climate conditions
111 during the past 1.8 Ma. However, they did not perform any trace element or
112 isotopic analyses. Finally, two samples of Sahara dust collected in southern
113 France were also analyzed.

114 The samples belong to two different types of loess deposits. The Western Europe
115 Loess samples are periglacial deposits that were produced during the last glacial
116 period by mechanical erosion of the crust followed by transport by wind over

117 limited distances [*Haase et al.*, 2007]. The situation is rather similar for the
118 Argentinian loess deposits whose origin is mainly the Andes [*Smith et al.*, 2003].
119 The Chinese and Tajikistan loess deposits represent much larger volumes and
120 have a very different origin: the materials come from large desert areas. For the
121 Chinese loess, particles come mainly from the deserts located Northwest in
122 Mongolia [*Sun*, 2002]; in southern Tajikistan, the particles originate from the
123 Karakum and Kyzylkum deserts located northwest in Turkmenistan, Uzbekistan
124 and Kazakhstan [*Ding et al.*, 2002]. In both cases, the deserts developed on
125 continental crust that formed over large periods of geological time [e.g., *Lee et al.*,
126 2011; *Yoshida*, 2012] and particles were transported over long distances by high-
127 energy winds to accumulate in protected areas [*Ding et al.*, 1999; *Ding et al.*,
128 2002; *Guo et al.*, 2002]. Consequently, they represent the average composition of
129 much larger crustal areas than the periglacial deposits. Finally, the dust blown
130 from the Sahara over Southern France does not constitute a real loess deposit
131 [*Grousset et al.*, 2003], but it provides valuable information on the average
132 composition of the largest desert area in the world.

133

134 **3 - Analytical techniques**

135 All samples were crushed using an agate mortar. Trace element concentrations
136 were obtained after dissolution in a HF-HClO₄ mixture using Parr bombs. The
137 complete procedure is that of Chauvel et al. [2011], but the dissolution time was
138 increased to insure complete dissolution of the very resistant minerals, an issue
139 particularly important when using the relationship between REE and Hf
140 concentrations and when measuring Hf isotopes. Both accuracy and
141 reproducibility of the data are estimated as better than 5% for most trace
142 elements, as shown by the analyses of international rocks standards and
143 duplicate analyses of samples (see Supplementary table).

144 Neodymium and hafnium were isolated from an aliquot of the solution prepared
145 for trace element analysis and using standard ion-chromatography as described
146 by Chauvel et al. [2011]. Total procedural blanks were less than 100 picograms
147 for both Nd and Hf. The Nd and Hf isotopic compositions were measured using
148 the Nu Plasma HR MC-ICP-MS at ENS Lyon. Mass bias corrections for Nd and Hf

149 isotopic compositions were performed using $^{146}\text{Nd}/^{144}\text{Nd} = 0.7219$ and
150 $^{179}\text{Hf}/^{177}\text{Hf} = 0.7325$ respectively. Over the course of analyses, daily averages
151 obtained for the Nd Ames-Rennes standard ranged between 0.511958 ± 19 and
152 0.511976 ± 14 , while those obtained for the Hf Ames-Grenoble standard ranged
153 between 0.282165 ± 9 and 0.282168 ± 19 . All isotopic ratios reported in Table 1
154 are normalized to the reference values of 0.511961 and 0.282160 as published
155 by Chauvel and Blichert-Toft [2001] and Chauvel et al. [2011]. Complete
156 duplicate analyses of several samples show that the reproducibility of isotopic
157 measurements is better than 100 ppm for both Nd and Hf isotopic ratios (Table
158 1).

159

160 **4 - Results**

161 New trace element data for the loess are provided in the Supplementary table.
162 Some samples had been previously analyzed for their trace element contents by
163 Gallet et al. [1998] and by Jahn et al. [2001] but these were reanalyzed because
164 some key elements (e.g., Hf) were not measured in many of these older studies.
165 The new values reported here are generally similar to those previously
166 published but there are notable exceptions. For example, the new
167 determinations of REE, Th, Zr and Hf concentrations are systematically higher
168 than those reported by Jahn et al. [2001] suggesting that dissolution of samples
169 in 2001 was incomplete, leaving some non-dissolved zircon and monazite grains
170 (see supplementary figure).

171 Figure 2 shows the trace element patterns obtained for all loess samples. As
172 previously shown by Gallet et al. [1996] and Jahn et al. [2001], the Chinese loess
173 are remarkably homogeneous with normalized trace element concentrations
174 close to the Upper Continental Crust values of Rudnick and Gao [2003] (see
175 Figure 2b). The new Tajikistan data shown in Figure 2c display similar features.
176 This is not the case, however, for the periglacial loess sampled in Western
177 Europe and shown in Figure 2a. The latter samples have much more variable
178 concentrations and they display large positive Zr-Hf anomalies, most probably
179 due to the presence of excess zircon. Finally, the Argentinian loess samples and
180 the two Sahara dust samples shown in Figure 2d have trace element patterns

181 generally parallel to the average upper continental crust (UCC) value, without
182 positive Zr-Hf anomalies, but with more variability.

183 The Nd and Hf isotopic compositions of all loess samples analyzed in this study
184 are listed in Table 1. The data are plotted in Figure 3 where they are compared to
185 data published in the literature for MORB, OIB, oceanic sediments and crustal
186 rocks. With the exception of the Argentinian samples, all loess define a restricted
187 range of ϵ_{Nd} and ϵ_{Hf} values (-10.3 ± 1.2 and -13.8 ± 4.2) and lie on the terrestrial
188 array of Vervoort et al. [2011] in the field of crustal materials. The Argentinian
189 loess have less negative values ($\epsilon_{Nd} = -1.7$ and $\epsilon_{Hf} = -2.8$), a feature attributed to
190 the abundance of Andean volcanic rocks in the source area [Gallet et al., 1998;
191 Smith et al., 2003].

192

193 **5 - Discussion**

194 Constraining the average composition of the continental crust is a very active
195 field of research [e.g., Armstrong, 1968; McCulloch and Wasserburg, 1978;
196 Armstrong, 1981; Allègre and Rousseau, 1984; Goldstein et al., 1984; Taylor and
197 McLennan, 1985; Condie, 1993; Wedepohl, 1995; Gallet et al., 1998; Vervoort et
198 al., 2000; Griffin et al., 2002; Rudnick and Gao, 2003; Hawkesworth and Kemp,
199 2006; Belousova et al., 2010; Hawkesworth et al., 2010; Dhuime et al., 2011;
200 Garçon et al., 2011]. Several studies have suggested average values for the upper
201 continental crust but these mainly focus on its major and trace element
202 composition (see Rudnick and Gao [2003] for a review). Knowing its radiogenic
203 isotopic compositions is also important since it provides constraints on the
204 timing of crust formation through geological time. Several Pb isotope
205 compositions have been suggested for the upper continental crust [e.g., Zartman
206 and Doe, 1981; Newsom et al., 1986; Rudnick and Goldstein, 1990; Garçon et al.,
207 2013b] as well as some average Nd model ages [Allègre and Rousseau, 1984;
208 Goldstein et al., 1984; Goldstein and Jacobsen, 1988; Jacobsen, 1988]. These show
209 that the continental crust formed, on average, about 1.8 to 2 Ga ago. Here, we will
210 use loess as a proxy to more precisely constrain the Nd and Hf isotopic
211 composition of average upper continental crust. We will then use these data to
212 re-evaluate when the upper crust separated from the mantle and use the

213 combined Nd and Hf isotopic data to constrain the Lu/Hf ratio of upper
214 continental crust. It could be argued that the sample set might not be
215 representative of average upper crust and we will demonstrate that it is.

216

217 **5.1 - Loess: an excellent proxy for the average upper continental crust Nd** 218 **isotopic ratio**

219 Loess has been widely used by Taylor and McLennan [1985] to establish the
220 average REE composition of the upper continental crust because these sediments
221 represent the average composition of large surface areas. Since the REE content
222 is representative of the upper continental crust, loess can be used to evaluate its
223 Nd isotopic composition [McCulloch and Wasserburg, 1978; Taylor et al., 1983;
224 Gallet et al., 1998].

225 The measured Nd isotopic ratios of nearly 50 loess samples are remarkably
226 uniform and define two groups (Figures 3 & 4). The first comprises only the
227 Argentinian loess and is relatively radiogenic with an average ϵ_{Nd} of -1.7. Gallet et
228 al. [1998] concluded that the unusual composition of these samples was due to
229 the overwhelming presence of recent volcanic products coming from the Andes
230 and could not be considered as representative of large areas of the upper
231 continental crust. We concur with their conclusion. The second group of samples
232 consists of all other analyzed loess samples (Figure 3). While the Chinese and
233 Tajikistan loess have indistinguishable isotopic compositions ($\epsilon_{Nd} = -9.82 \pm 0.44$
234 and $\epsilon_{Nd} = -9.46 \pm 0.36$, respectively), the two Sahara dusts have lower ϵ_{Nd} at -12.4.
235 Finally, the Western European loess are more heterogeneous and average at ϵ_{Nd}
236 = -11.25 ± 1.28 . We attribute this larger range of isotopic compositions to
237 processes acting during the formation of periglacial loess, when relatively small
238 volumes of material were produced by erosion of proximal sources during the
239 last glacial period. Such small volumes of glacial sediments were not well mixed
240 by long distance transport and their composition is a function of the diversity of
241 local terranes in Western Europe. In contrast, the Tajikistan and the Chinese
242 loess are remarkably homogeneous, a feature consistent with their origin as dust
243 blown from large desert areas [Ding et al., 1999; Ding et al., 2002]. Nevertheless,

244 taken together, all these samples define a well-constrained average at $\epsilon_{Nd}=-$
245 10.3 ± 1.2 (1σ) (see inset of Figure 3).

246 Given the large number of Chinese and Tajikistan samples in our data set, it could
247 be argued that our average ϵ_{Nd} value is only representative of the upper
248 continental crust present in Russia and Central Asia. However, similar ϵ_{Nd} values
249 have been reported for all sorts of other areas in the world: The Carpathian loess
250 deposits in Eastern Europe have an average ϵ_{Nd} value at -10.21 ± 0.34 [Újvári *et*
251 *al.*, 2012] and a placer deposit that averages the area drained by the Rhone River
252 in Western Europe has an ϵ_{Nd} value of -9.3 [Garçon *et al.*, 2011]. This suggests
253 that most of the European continent has an ϵ_{Nd} value at about -10 . The only two
254 US loess samples analyzed for Nd isotopes have lower values at -13 and -15
255 [Taylor *et al.*, 1983] which might indicate that the American upper crust could
256 have a different average value. However, the ϵ_{Nd} values reported by Goldstein *et*
257 *al.* [1984] and Goldstein and Jacobsen [1988] for particulates collected on major
258 rivers from the American continent do not confirm these low values but provide
259 a range between -20.8 and -4.4 . Worldwide aerosols can also be used to estimate
260 the composition of exposed continental crust. Grousset and Biscaye [2005]
261 compiled the existing data and showed that aerosols have much more variable
262 compositions than loess or river particulates, but they could estimate that the
263 world mean ϵ_{Nd} value was around -11 [Grousset and Biscaye, 2005]. Finally,
264 Goldstein *et al.* [1984] analyzed a large number of river sediments and aeolian
265 dusts from various continents and provided an average ϵ_{Nd} value at -11.4 ± 4 for
266 all these deposits. Given the similarity of all the values listed above, we suggest
267 that our estimate ($\epsilon_{Nd}=-10.3$) is probably accurate and representative of
268 continental crust exposed today at the surface of the Earth. Estimating the
269 uncertainty is more difficult. Here we use the 1σ error based on our data set
270 (± 1.2) but we acknowledge that with a larger set of samples, the value could
271 change.

272

273 **5.2 - Loess: also a good proxy for the average upper continental crust Hf**
274 **isotopic ratio**

275 Several authors have argued that the Zr and Hf contents of loess should not be
276 used as analogues for their source [*Taylor et al.*, 1983; *Barth et al.*, 2000; *Rudnick*
277 *and Gao*, 2003]. These arguments are based on the observation that the loess
278 that they had studied had a very large excess of Zr and Hf relative to the REE, a
279 feature attributed to the presence of excess zircons. All the samples that they
280 studied, however, are periglacial loess sediments. Our Western European loess
281 samples have the same large positive anomaly in Zr and Hf (see Figure 2) and we
282 argue that many or all periglacial loess deposits contain this feature. In contrast,
283 the Tajikistan, Chinese and Argentinian loess deposits as well as the Sahara dusts
284 either have no anomaly or a slight negative anomaly (Figure 2). Since zircons are
285 rich in Hf and have usually very unradiogenic Hf isotopes, their presence has
286 strong impact on the whole rock Hf isotopic composition. As a result, the
287 measured Hf isotopic ratios reported in the Table 1 for the Western European
288 loess cannot be directly used to establish the average composition of the upper
289 continental crust. It is, however, possible to correct for the “zircon effect” by
290 using the relationship between Nd/Hf and $\Delta\epsilon_{\text{Hf}}$ (the vertical deviation from the
291 terrestrial array as defined by *Carpentier et al.* [2009]) as shown in Figure 4.
292 Nd/Hf is well constrained in all estimates of upper continental crust, while $\Delta\epsilon_{\text{Hf}}$ is
293 a good measure of mineralogical sorting during sediment formation [*Carpentier*
294 *et al.*, 2009; *Vervoort et al.*, 2011; *Garçon et al.*, 2013a]. In Figure 4, loess deposits
295 define a positive correlation. The Western Europe loess have low Nd/Hf (i.e.,
296 positive Hf anomalies), lie below the terrestrial array of *Vervoort et al.* [2011]
297 and have negative $\Delta\epsilon_{\text{Hf}}$ values, as expected by the presence of excess old zircons.
298 In contrast, the Tajikistan loess samples have relatively high Nd/Hf (i.e., slight
299 negative Hf anomalies) and slightly positive $\Delta\epsilon_{\text{Hf}}$ values, as expected for
300 sediments deficient in zircon relative to their crustal source [*Carpentier et al.*,
301 2009; *Vervoort et al.*, 2011; *Garçon et al.*, 2013a]. The Chinese and Argentinian
302 loess have compositions that plot in between these two end members. Using the
303 values recommended for the Nd/Hf ratio of upper continental crust, we can
304 therefore estimate the $\Delta\epsilon_{\text{Hf}}$ value for average upper continental crust. The most
305 recent estimation of $(\text{Nd}/\text{Hf})_{\text{UCC}}$ provided by *Rudnick and Gao* [2003] constrains
306 the $\Delta\epsilon_{\text{Hf}}$ value for upper continental crust at +1.6 with an error of less than ± 2 ,
307 based on the range of estimated $(\text{Nd}/\text{Hf})_{\text{UCC}}$ (see Figure 4).

308 This $\Delta\epsilon_{\text{Hf}}$ value translates into an ϵ_{Hf} value of -13.2 ± 2 (1σ) using the average ϵ_{Nd}
309 value of -10.3 determined above and the terrestrial array equation of Vervoort et
310 al. [2011] ($\epsilon_{\text{Hf}} = 1.55 \cdot \epsilon_{\text{Nd}} + 1.21$). Such value is not identical to the average of all
311 loess measurements (-13.8 ± 4.2) but it is similar and the error on the average is
312 smaller. These ϵ values correspond to a $^{143}\text{Nd}/^{144}\text{Nd}$ of 0.512102 ± 67 and a
313 $^{176}\text{Hf}/^{177}\text{Hf}$ of 0.282412 ± 56 (see Table 2).

314 The combined Nd and Hf isotopic values for average upper continental crust
315 define the point shown as a red star in Figure 3 at $\epsilon_{\text{Nd}} = -10.3 \pm 1.2$ (1σ) and $\epsilon_{\text{Hf}} = -$
316 13.2 ± 2 (1σ), an average that plots, within error, on the terrestrial array thereby
317 supporting the long-standing observation that the parent-daughter ratios Sm/Nd
318 and Lu/Hf are coupled during magmatic processes both in the mantle and the
319 crust. It also provides a value for the average upper continental crust, a value
320 that is very useful in modeling how the continents formed.

321

322 **5.3 - Nd model age of upper continental crust**

323 To model the average formation age of the upper continental crust, we need
324 well-constrained values not only for Nd and Hf isotopic compositions but also for
325 Sm/Nd and Lu/Hf ratios. Data listed in Table 1 show that both the loess Nd
326 isotopic compositions and their $^{147}\text{Sm}/^{144}\text{Nd}$ ratios (0.1193 ± 0.0026 , recalculated
327 using the Sm and Nd concentrations) are extremely constant. This feature arises
328 from the uniform Sm/Nd ratio of most crustal minerals [*Taylor and McLennan,*
329 *1981; Goldstein et al., 1984; Taylor and McLennan, 1985; Garçon et al., 2011*].
330 When compared to the $^{147}\text{Sm}/^{144}\text{Nd}$ ratio recalculated from previously published
331 UCC estimates [*Taylor and McLennan, 1985; Condie, 1993; Gao et al., 1998;*
332 *Rudnick and Gao, 2003*], our value is slightly higher (0.1193 vs. ≈ 0.1050) a
333 feature that may be related to the poor precision of the Sm and Nd concentration
334 estimates used in these publications (typically 10%, see Table 2). Our value is
335 similar, however, to values proposed by Jahn and Condie [*Jahn and Condie, 1995*]
336 and in studies when the $^{147}\text{Sm}/^{144}\text{Nd}$ was determined with better precision
337 [*McCulloch and Wasserburg, 1978; Allègre and Rousseau, 1984; Goldstein et al.,*
338 *1984*]. Using this value for $^{147}\text{Sm}/^{144}\text{Nd}$ (0.1193 ± 0.0026), our UCC estimate for

339 $^{143}\text{Nd}/^{144}\text{Nd}$, the depleted mantle values listed in Table 2 and the following
340 equation,

$$T_{\text{DM}} = \text{Log} \left(\frac{\left(\frac{^{143}\text{Nd}}{^{144}\text{Nd}} \right)_{\text{UCC}} - \left(\frac{^{143}\text{Nd}}{^{144}\text{Nd}} \right)_{\text{DM}}}{\left(\frac{^{147}\text{Sm}}{^{144}\text{Nd}} \right)_{\text{UCC}} - \left(\frac{^{147}\text{Sm}}{^{144}\text{Nd}} \right)_{\text{DM}}} - 1 \right) / \lambda$$

341 (with $\lambda=6.54 \cdot 10^{-12} \text{ year}^{-1}$) we can calculate a model age for the extraction of the
342 crust from the depleted mantle.

343 We obtain a Nd model age of $1.82 \pm 0.07 \text{ Ga}$ (1σ) for the separation of crust from
344 the mantle. Such value falls within the range of previous estimates based on Nd
345 isotopes [e.g., *Allègre and Rousseau, 1984; Goldstein et al., 1984; Hawkesworth*
346 *and Kemp, 2006*], but has a much smaller error than previous estimates.

347 The calculated model age depends heavily on the chosen parameters for the
348 depleted mantle source. Here, we consider that depletion started at the
349 beginning of Earth history and we chose a very depleted mantle (see Table 2).
350 Other authors prefer more subdued values. For example, Gale et al. [2013]
351 recently provided an estimate based on the average composition of MORB while
352 Dhuime et al. [2011] suggested that the source of newly formed continental crust
353 was less depleted than the MORB mantle (see Table 2). When these references
354 are used, we calculate that the Nd model age of upper continental crust would be
355 200 Ma younger. An extra complication has been introduced recently by Jackson
356 and Carlson's [2012] suggestion that the Earth has a superchondritic
357 composition. Gale et al. [2013] already discussed the issue and showed that a
358 serious problem occurs because the present-day isotopic composition of a
359 superchondritic Earth is identical to their estimate of present-day depleted
360 mantle. Indeed, this leaves no space for the development of a mantle that had
361 become depleted as a consequence of the extraction of enriched continental
362 crust. If we accept that the Earth is superchondritic and that the depleted mantle
363 is more depleted than suggested by Gale et al. [2013], with, for example, a Nd
364 isotopic composition similar to our chosen estimate (see Table 2), then the entire
365 mantle would have to be depleted to compensate for the extraction of the
366 continental crust.

367

368 5.4 - $^{176}\text{Lu}/^{177}\text{Hf}$ ratio of upper continental crust and Hf model age

369 To establish the average Hf model age of the upper continental crust is not as
370 straightforward as for Nd because the $^{176}\text{Lu}/^{177}\text{Hf}$ ratio of continental crust is
371 poorly constrained, yet has a major impact on the calculations. In Table 2, we list
372 estimates of $^{176}\text{Lu}/^{177}\text{Hf}_{\text{UCC}}$ that have been suggested in the literature. The
373 $^{176}\text{Lu}/^{177}\text{Hf}$ values calculated using upper crustal Lu and Hf contents range
374 mostly from 0.0057 to 0.0106 [Shaw *et al.*, 1967; Shaw *et al.*, 1976; Taylor and
375 McLennan, 1985; Condie, 1993; Wedepohl, 1995; Gao *et al.*, 1998; Rudnick and
376 Gao, 2003] but higher values have also been suggested: Goodge and Vervoort
377 [2006] suggest a $^{176}\text{Lu}/^{177}\text{Hf}$ ratio of 0.0150 for new Proterozoic crust, while
378 Hawkesworth *et al.* [2010] suggested a value of 0.0159 on the basis of over 7000
379 measurements of granitoids. Finally, Condie and co-workers [Condie *et al.*, 2011]
380 suggest a value as high as 0.020. The range of suggested values is therefore very
381 large.

382 Unfortunately, the measured $^{176}\text{Lu}/^{177}\text{Hf}$ ratios of the loess samples cannot be
383 used to estimate the $^{176}\text{Lu}/^{177}\text{Hf}$ of the upper continental crust because loess
384 deposits are affected by sedimentary processes that sort minerals eroded from
385 crustal rocks. In contrast to their generally uniform $^{147}\text{Sm}/^{144}\text{Nd}$ ratios, all
386 minerals do not have similar $^{176}\text{Lu}/^{177}\text{Hf}$ ratios, and their relative proportions
387 strongly influence the whole-rock $^{176}\text{Lu}/^{177}\text{Hf}$ ratio, which might be quite
388 different from that of the crustal precursor. One mineral, zircon, is particularly
389 important because it dominates the whole-rock $^{176}\text{Lu}/^{177}\text{Hf}$ ratio with its very
390 high Hf content and its extremely low $^{176}\text{Lu}/^{177}\text{Hf}$ ratio. In addition, it is very
391 resistant to alteration processes and survives even extreme weathering. If a high
392 proportion of old zircon is retained in a loess deposit, then the whole rock has
393 low $^{176}\text{Lu}/^{177}\text{Hf}$ and unradiogenic $^{176}\text{Hf}/^{177}\text{Hf}$, as is the case with the Western
394 European loess deposits (see Table 1 and Figure 4). In contrast, if the proportion
395 of zircon is lower, as is the case for the Tajikistan loess samples, then the
396 $^{176}\text{Lu}/^{177}\text{Hf}$ is higher and $^{176}\text{Hf}/^{177}\text{Hf}$ is more radiogenic. Thus, the large range of
397 $^{176}\text{Lu}/^{177}\text{Hf}$ ratios reported in loess deposits is likely controlled by sedimentary
398 sorting processes and these values cannot be considered as representative of the
399 $^{176}\text{Lu}/^{177}\text{Hf}$ ratio of the crustal precursors. We therefore use a different

400 approach that combines the constraints provided by the Sm-Nd and Lu-Hf
401 isotopic systems to determine the best estimate for the upper continental crust
402 Lu/Hf ratio.

403 In Figure 5, we plot Hf model ages of individual loess samples as a function of
404 their Nd model age. For each sample, we use the measured $^{147}\text{Sm}/^{144}\text{Nd}$ and
405 $^{143}\text{Nd}/^{144}\text{Nd}$ ratios as well as the depleted mantle values shown with an asterisk
406 in Table 2. To calculate the Hf crustal model ages, we used the measured
407 $^{176}\text{Hf}/^{177}\text{Hf}$ ratios together with a range of $^{176}\text{Lu}/^{177}\text{Hf}$ ratios as published for
408 upper continental crust, and the depleted mantle values shown with an asterisk
409 in Table 2. Because the range of possible $^{176}\text{Lu}/^{177}\text{Hf}$ ratios in average upper
410 crust (between 0.0057 and 0.0200, see Table 2) is very large, it introduces a very
411 large range of possible Hf model ages $T_{\text{DM}}(\text{Hf})$ (shown by vertical lines in Figure
412 5). If the upper crust has a high $^{176}\text{Lu}/^{177}\text{Hf}$ ratio of 0.0200, as suggested by
413 Condie et al. [2011], then the $T_{\text{DM}}(\text{Hf})$ of all loess (excluding the Argentinian
414 loess) averages 2.47 ± 0.13 Ga, a value that is 600 Ma older than the average Nd
415 model age (1.82 ± 0.07 Ga); if the crustal $^{176}\text{Lu}/^{177}\text{Hf}$ ratio is 0.0159, as suggested
416 by Hawkesworth et al. [2010], then the $T_{\text{DM}}(\text{Hf})$ average at 2.05 ± 0.11 Ga, still
417 over 200 Ma older than the average Nd model age. In contrast, using a low
418 $^{176}\text{Lu}/^{177}\text{Hf}$ ratio at 0.0057 provides much younger Hf model ages (1.45 ± 0.08
419 Ga). Finally, a $^{176}\text{Lu}/^{177}\text{Hf}$ ratio of 0.0083, as suggested by Rudnick and Gao
420 [2003], gives an average Hf model age of 1.57 ± 0.09 Ga.

421 Considering the overall geochemical behavior of REE and Zr-Hf during magmatic
422 and sedimentary processes [Vervoort and Patchett, 1996; Vervoort and Blichert-
423 Toft, 1999; Vervoort et al., 1999; Chauvel et al., 2008; Carpentier et al., 2009;
424 Vervoort et al., 2011], it seems unlikely that the Nd model age of upper
425 continental crust should be older than its Hf model age. The opposite is, in fact,
426 much more likely because most Hf present in crustal materials is sequestered in
427 zircon, a mineral phase that is extremely robust during alteration and reworking
428 of continental crust.

429 To constrain the $^{176}\text{Lu}/^{177}\text{Hf}$ ratio of the upper continental crust, we assume here
430 that $T_{\text{DM}}(\text{Hf})$ and $T_{\text{DM}}(\text{Nd})$ should be identical for each individual loess and dust
431 sample and we calculate the necessary $^{176}\text{Lu}/^{177}\text{Hf}$ ratio for each individual

432 sample. Results of the calculation are shown in Figure 6 where they are also
433 compared to the range of suggested values from literature. On average, we
434 estimate that the $^{176}\text{Lu}/^{177}\text{Hf}$ ratio of upper continental crust is 0.0125 ± 0.0018
435 (1σ).

436 In summary, the loess data suggest that the average model age of upper
437 continental crust is 1.82 ± 0.07 Ga (1σ) based on Nd isotopes. Assuming that Hf
438 model ages cannot be any younger than Nd model ages, the loess data also
439 provide constraints on the $^{176}\text{Lu}/^{177}\text{Hf}$ ratio of upper continental crust, which
440 cannot be smaller than 0.00125 ± 0.0018 , the value that corresponds to
441 concordant $T_{\text{DM}}(\text{Hf})$ and $T_{\text{DM}}(\text{Nd})$ ages. Higher values, such as those suggested
442 previously by other authors [*Goodge and Vervoort, 2006; Hawkesworth et al.,*
443 *2010*] are also plausible, but would result in an average upper crust $T_{\text{DM}}(\text{Hf})$ age
444 over 200 Ma older than the $T_{\text{DM}}(\text{Nd})$ age.

445

446 **6 - Conclusions**

447 Our Nd-Hf isotopic study of a large number of loess samples provides new
448 constraints on the average isotopic composition of the upper continental crust.
449 We estimate that present-day upper continental crust has the following
450 characteristics: $^{143}\text{Nd}/^{144}\text{Nd} = 0.512101\pm 60$ and $^{176}\text{Hf}/^{177}\text{Hf} = 0.282412\pm 60$. Using
451 the bulk silicate Earth values determined by Bouvier et al. [2008], these isotopic
452 ratios translate into $\epsilon_{\text{Nd}} = -10.3\pm 1.2$ ($\pm 1\sigma$) and $\epsilon_{\text{Hf}} = -13.2\pm 2$ ($\pm 1\sigma$) and fall within
453 error on the terrestrial array of Vervoort et al. [2011].

454 The uniform $^{147}\text{Sm}/^{144}\text{Nd}$ ratio (0.1193 ± 0.0026) of loess deposits can also be
455 considered as representative of the upper continental crust value. Combining the
456 parent/daughter ratio with the average Nd isotopic composition, we calculate
457 that the average Nd model age of upper continental crust is 1.82 ± 0.07 Ga.

458 Finally, we constrain the $^{176}\text{Lu}/^{177}\text{Hf}$ ratio of the upper continental crust using
459 the relationship between Hf and Nd isotopes. Our preferred estimate
460 corresponds to 0.0125 ± 0.0018 , a value that is significantly higher than most
461 previous estimates but lower than the ratio suggested by Goodge and Vervoort
462 [2006] and Hawkesworth et al. [2010]. We emphasize that 0.0125 represents the

463 lower limit for $^{176}\text{Lu}/^{177}\text{Hf}$ because any lower estimate makes the Hf model ages
464 younger than the Nd model ages, a very unlikely situation given the geochemical
465 behavior of Hf and REE. The impact of this new $^{176}\text{Lu}/^{177}\text{Hf}$ ratio on crustal
466 differentiation ages of zircon populations such as those calculated by numerous
467 authors [e.g., *Griffin et al.*, 2002; *Harrison et al.*, 2005; *Kemp et al.*, 2007; *Blichert-*
468 *toft and Albarède*, 2008; *Wang et al.*, 2009; *Belousova et al.*, 2010; *Kemp et al.*,
469 2010; *Yao et al.*, 2011; *Iizuka et al.*, 2013] is quite variable, but the ages can be
470 younger by up to 500 Ma in the most extreme cases.

471

472 **7 - Acknowledgments:** We would like to thank Sylvain Gallet who provided the
473 loess samples that he studied during his PhD. Thank also to Philippe Telouk in
474 Lyon who always makes sure that the MC-ICP-MS behaves properly when we
475 come to use it. Special thanks to Jeff Vervoort and Nick Arndt who read and made
476 comments on a first draft of this manuscript, to an anonymous reviewer and to
477 Roberta Rudnick who made very constructive comments that helped clarify the
478 discussion and to Mark Harrison for his editorial job. Financial support for this
479 work came from general funds from the CNRS and the University of Grenoble.

480

481

482

483 **8 - References:**

484 Albarède, F., A. Simonetti, J. D. Vervoort, J. Blichert-Toft, and W. Abouchami
485 (1998), A Hf-Nd isotopic correlation in ferromanganese nodules, *Geoph. Res. Lett.*,
486 25(20), 3895-3898.
487 Allègre, C. J., and D. Rousseau (1984), The growth of the continents through
488 geological time studied by Nd isotope analysis of shales, *Earth Planet. Sci. Lett.*,
489 67, 19-34.
490 Armstrong, R. L. (1968), A model for the evolution of strontium and lead isotopes
491 in a dynamic earth, *Review of Geophysics*, 6, 175-199.
492 Armstrong, R. L. (1981), Radiogenic isotopes: the case for crustal recycling on a
493 near-steady-state no-continental growth earth, *Phil. Trans. Roy. Soc. Lond.*, 301,
494 443-472.
495 Barth, M. G., W. F. McDonough, and R. L. Rudnick (2000), Tracking the budget of
496 Nb and Ta in the continental crust, *Chem. Geol.*, 165(3-4), 197-213.
497 Bayon, G., K. W. Burton, G. Soulet, N. Vigier, B. Dennielou, J. Etoubleau, E.
498 Ponzevera, C. R. German, and R. W. Nesbitt (2009), Hf and Nd isotopes in marine

499 sediments: Constraints on global silicate weathering, *Earth Planet. Sci. Lett.*,
500 277(3-4), 318-326.

501 Belousova, E. A., Y. A. Kostitsyn, W. L. Griffin, G. C. Begg, S. Y. O'Reilly, and N. J.
502 Pearson (2010), The growth of the continental crust: Constraints from zircon Hf-
503 isotope data, *Lithos*, 119(3-4), 457-466.

504 BenOthman, D., W. M. White, and P. J. Patchett (1989), The geochemistry of
505 marine sediments, island arc magma genesis, and crust-mantle recycling, *Earth*
506 *Planet. Sci. Lett.*, 94, 1-21.

507 Blichert-toft, J., and F. Albarède (2008), Hafnium isotopes in Jack Hills zircons
508 and the formation of the Hadean crust, *Earth Planet. Sci. Lett.*, 265, 686-702.

509 Bouvier, A., J. D. Vervoort, and P. J. Patchett (2008), The Lu-Hf and Sm-Nd
510 isotopic composition of CHUR: Constraints from unequilibrated chondrites and
511 implications for the bulk composition of terrestrial planets, *Earth Planet. Sci. Lett.*,
512 273(1-2), 48-57.

513 Carpentier, M., C. Chauvel, and N. Mattielli (2008), Pb-Nd isotopic constraints on
514 sedimentary input into the Lesser Antilles arc system, *Earth Planet. Sci. Lett.*,
515 272(1-2), 199-211.

516 Carpentier, M., C. Chauvel, R. C. Maury, and N. Mattielli (2009), The "zircon effect"
517 as recorded by the chemical and Hf isotopic compositions of Lesser Antilles
518 forearc sediments, *Earth Planet. Sci. Lett.*, 287(1-2), 86-99.

519 Chauvel, C., and J. Blichert-Toft (2001), A hafnium isotope and trace element
520 perspective on melting of the depleted mantle, *Earth Planet. Sci. Lett.*, 190, 137-
521 151.

522 Chauvel, C., S. Bureau, and C. Poggi (2011), Comprehensive Chemical and Isotopic
523 Analyses of Basalt and Sediment Reference Materials, *Geostandards and*
524 *Geoanalytical Research*, 35(1), 125-143.

525 Chauvel, C., J.-C. Marini, T. Plank, and J. N. Ludden (2009), Hf-Nd input flux in the
526 Izu-Mariana subduction zone and recycling of subducted material in the mantle,
527 *Geochem. Geophys. Geosyst.*, 10, Q01001, doi: [10.1029/2008GC002101](https://doi.org/10.1029/2008GC002101).

528 Chauvel, C., E. Lewin, M. Carpentier, N. T. Arndt, and J.-C. Marini (2008), Role of
529 recycled oceanic basalt and sediment in generating the Hf-Nd mantle array,
530 *Nature Geosci.*, 1(1), 64-67.

531 Condie, K. C. (1993), Chemical composition and evolution of the upper
532 continental crust: Contrasting results from surface samples and shales, *Chem.*
533 *Geol.*, 104, 1-37.

534 Condie, K. C., M. E. Bickford, R. C. Aster, E. Belousova, and D. W. Scholl (2011),
535 Episodic zircon ages, Hf isotopic composition, and the preservation rate of
536 continental crust, *Geol. Soc. Am. Bull.*, 123(5-6), 951-957.

537 David, K., M. Frank, R. K. O'Nions, N. S. Belshaw, and J. W. Arden (2001), The Hf
538 isotope composition of global seawater and the evolution of Hf isotopes in the
539 deep Pacific Ocean from Fe-Mn crusts, *Chem. Geol.*, 178, 23-42.

540 Dhuime, B., C. J. Hawkesworth, and P. Cawood (2011), When continents formed,
541 *Science*, 331, 154-155.

542 Ding, Z., J. Sun, N. W. Rutter, D. Rokosh, and T. Liu (1999), Changes in Sand
543 Content of Loess Deposits along a North-South Transect of the Chinese Loess
544 Plateau and the Implications for Desert Variations, *Quaternary Research*, 52(1),
545 56-62.

546 Ding, Z. L., V. Ranov, S. L. Yang, A. Finaev, J. M. Han, and G. A. Wang (2002), The
547 loess record in southern Tajikistan and correlation with Chinese loess, *Earth*
548 *Planet. Sci. Lett.*, *200*(3-4), 387-400.

549 Gale, A., C. A. Dalton, C. H. Langmuir, Y. Su, and J.-G. Schilling (2013), The mean
550 composition of ocean ridge basalts, *Geochem. Geophys. Geosyst.*, n/a-n/a.

551 Gallet, S., B.-M. Jahn, and M. Torii (1996), Geochemical characterization of the
552 Luochuan loess-paleosol sequence, China, and paleoclimatic implications, *Chem.*
553 *Geol.*, *133*, 67-88.

554 Gallet, S., B.-M. Jahn, B. V. V. Lanoë, A. Dia, and E. Rossello (1998), Loess
555 geochemistry and its implications for particle origin and composition of the
556 upper continental crust, *Earth Planet. Sci. Lett.*, *156*, 157-172.

557 Gao, S., T.-C. Luo, B.-R. Zhang, H.-F. Zhang, Y.-w. Han, Z.-D. Zhao, and Y.-K. Hu
558 (1998), Chemical composition of the continental crust as revealed by studies in
559 East China, *Geochim. Cosmochim. Acta*, *62*(11), 1959-1975.

560 Garçon, M., C. Chauvel, and S. Bureau (2011), Beach placer, a proxy for the
561 average Nd and Hf isotopic composition of a continental area, *Chem. Geol.*, *287*(3-
562 4), 182-192.

563 Garçon, M., C. Chauvel, C. France-Lanord, P. Huyghe, and J. Lavé (2013a),
564 Continental sedimentary processes decouple Nd and Hf isotopes, *Geochim.*
565 *Cosmochim. Acta*, *121*(0), 177-195.

566 Garçon, M., C. Chauvel, C. France-Lanord, M. Limonta, and E. Garzanti (2013b),
567 Removing the “heavy mineral effect” to obtain a new Pb isotopic value for the
568 upper crust, *Geochem. Geophys. Geosyst.*, 10.1002/ggge.20219.

569 Godfrey, L. V., D.-C. Lee, W. F. Sangrey, A. N. Halliday, V. J. M. Salters, J. R. Hein,
570 and W. M. White (1997), The Hf isotopic composition of ferromanganese nodules
571 and crusts and hydrothermal manganese deposits: Implications for seawater Hf,
572 *Earth Planet. Sci. Lett.*, *151*, 91-105.

573 Goldstein, S. J., and S. B. Jacobsen (1988), Nd and Sr isotopic systematics of river
574 water suspended material: implications for crustal evolution, *Earth Planet. Sci.*
575 *Lett.*, *87*(3), 249-265.

576 Goldstein, S. L., R. K. O’Nions, and P. J. Hamilton (1984), A Sm-Nd isotopic study
577 of atmospheric dusts and particulates from major river systems, *Earth Planet. Sci.*
578 *Lett.*, *70*, 221-236.

579 Goodge, J. W., and J. D. Vervoort (2006), Origin of Mesoproterozoic A-type
580 granites in Laurentia: Hf isotope evidence, *Earth Planet. Sci. Lett.*, *243*(3-4), 711-
581 731.

582 Griffin, W. L., X. Wang, S. E. Jackson, N. J. Pearson, S. Y. O’Reilly, X. Xu, and X. Zhou
583 (2002), Zircon chemistry and magma mixing, SE China: In-situ analysis of Hf
584 isotopes, Tonglu and Pingtan igneous complexes, *Lithos*, *61*(3-4), 237-269.

585 Grousset, F. E., and P. E. Biscaye (2005), Tracing dust sources and transport
586 patterns using Sr, Nd and Pb isotopes, *Chem. Geol.*, *222*(3-4), 149-167.

587 Grousset, F. E., P. Ginoux, A. Bory, and P. E. Biscaye (2003), Case study of a
588 Chinese dust plume reaching the French Alps, *Geoph. Res. Lett.*, *30*(6), 1277.

589 Guo, Z. T., W. F. Ruddiman, Q. Z. Hao, H. B. Wu, Y. S. Qiao, R. X. Zhu, S. Z. Peng, J. J.
590 Wei, B. Y. Yuan, and T. S. Liu (2002), Onset of Asian desertification by 22 Myr ago
591 inferred from loess deposits in China, *Nature*, *416*, 159-163.

592 Haase, D., J. Fink, G. Haase, R. Ruske, M. Pécsi, H. Richter, M. Altermann, and K. D.
593 Jäger (2007), Loess in Europe—its spatial distribution based on a European
594 Loess Map, scale 1:2,500,000, *Quaternary Science Reviews*, *26*(9-10), 1301-1312.

595 Harrison, T. M., J. Blichert-Toft, W. Müller, F. Albarede, P. Holden, and S. J. Mojzsis
 596 (2005), Heterogeneous Hadean Hafnium: Evidence of Continental Crust at 4.4 to
 597 4.5 Ga, *Science*, *310*(5756), 1947-1950.
 598 Hawkesworth, C. J., and A. I. S. Kemp (2006), Evolution of the continental crust,
 599 *Nature*, *443*(7113), 811-817.
 600 Hawkesworth, C. J., B. Dhuime, A. B. Pietranik, P. A. Cawood, A. I. S. Kemp, and C.
 601 D. Storey (2010), The generation and evolution of the continental crust, *Journal*
 602 *of the Geological Society*, *167*(2), 229-248.
 603 Iizuka, T., I. H. Campbell, C. M. Allen, J. B. Gill, S. Maruyama, and F. Makoka (2013),
 604 Evolution of the African continental crust as recorded by U-Pb, Lu-Hf and O
 605 isotopes in detrital zircons from modern rivers, *Geochim. Cosmochim. Acta*,
 606 *107*(0), 96-120.
 607 Jackson, M. G., and R. W. Carlson (2012), Homogeneous superchondritic
 608 $^{142}\text{Nd}/^{144}\text{Nd}$ in the mid-ocean ridge basalt and ocean island basalt mantle,
 609 *Geochem. Geophys. Geosyst.*, *13*(6), Q06011.
 610 Jacobsen, S. B. (1988), Isotopic constraints on crustal growth and recycling, *Earth*
 611 *Planet. Sci. Lett.*, *90*(3), 315-329.
 612 Jahn, B.-M., and K. C. Condie (1995), Evolution of the Kaapvaal Craton as viewed
 613 from geochemical and Sm-Nd isotopic analyses of intracratonic pelites, *Geochim.*
 614 *Cosmochim. Acta*, *59*(11), 2239-2258.
 615 Jahn, B.-M., S. Gallet, and J. Han (2001), Geochemistry of the Xining, Xifeng and
 616 Jixian sections, Loess Plateau of China: eolian dust provenance and paleosol
 617 evolution during the last 140 Ka, *Chem. Geol.*, *178*, 71-94.
 618 Kemp, A. I. S., C. J. Hawkesworth, G. L. Foster, B. A. Paterson, J. D. Woodhead, J. M.
 619 Hergt, C. M. Gray, and M. J. Whitehouse (2007), Magmatic and Crustal
 620 Differentiation History of Granitic Rocks from Hf-O Isotopes in Zircon, *Science*,
 621 *315*(5814), 980-983.
 622 Kemp, A. I. S., S. A. Wilde, C. J. Hawkesworth, C. D. Coath, A. Nemchin, R. T.
 623 Pidgeon, J. D. Vervoort, and S. A. DuFrane (2010), Hadean crustal evolution
 624 revisited: New constraints from Pb-Hf isotope systematics of the Jack Hills
 625 zircons, *Earth Planet. Sci. Lett.*, *296*(1-2), 45-56.
 626 Lee, C.-T. A., P. Luffi, and E. J. Chin (2011), Building and Destroying Continental
 627 Mantle, *Annual Review of Earth and Planetary Sciences*, *39*(1), 59-90.
 628 McCulloch, M. T., and G. J. Wasserburg (1978), Sm-Nd and Rb-Sr Chronology of
 629 Continental Crust Formation, *Science*, *200*(4345), 1003-1011.
 630 McLennan, S. M., S. R. Taylor, M. T. M. Culloch, and J. B. Maynard (1990),
 631 Geochemical and Nd-Sr isotopic composition of deep-sea turbidites: crustal
 632 evolution and plate tectonic associations, *Geochim. Cosmochim. Acta*, *54*, 2015-
 633 2050.
 634 Newsom, H. E., W. M. White, K. P. Jochum, and A. W. Hofmann (1986), Siderophile
 635 and chalcophile element abundances in oceanic basalts, Pb isotope evolution and
 636 growth of the Earth's core, *Earth Planet. Sci. Lett.*, *80*, 299-313.
 637 Pearce, J. A., P. D. Kempton, G. M. Nowell, and S. R. Noble (1999), Hf-Nd element
 638 and isotope perspective on the nature and provenance of mantle and subduction
 639 components in Western Pacific arc-basin systems, *J. Petrol.*, *40*(11), 1579-1611.
 640 Peucat, J.-J., P. Jegouzo, P. Vidal, and J. Bernard-Griffiths (1988), Continental crust
 641 formation seen through the Sr and Nd isotope systematics of S-type granites in
 642 the Hercynian belt of western France, *Earth Planet. Sci. Lett.*, *88*, 60-68.

643 Prytulak, J., J. D. Vervoort, T. Plank, and C. Yu (2006), Astoria Fan sediments,
644 DSDP site 174, Cascadia Basin: Hf-Nd-Pb constraints on provenance and outburst
645 flooding, *Chem. Geol.*, *233*, 276-292.

646 Rudnick, R. L., and S. L. Goldstein (1990), The Pb isotopic composition of lower
647 crustal xenoliths and the evolution of lower crustal Pb, *Earth Planet. Sci. Lett.*, *98*,
648 192-207.

649 Rudnick, R. L., and S. Gao (2003), 3.01 - Composition of the Continental Crust, in
650 *Treatise on Geochemistry*, edited by D. H. Editors-in-Chief: Heinrich and K. T. Karl,
651 pp. 1-64, Pergamon, Oxford.

652 Salters, V. J. M., and A. Stracke (2004), Composition of the depleted mantle,
653 *Geochemistry Geophysics Geosystems*, *5*.

654 Shaw, D. M., J. Dostal, and R. R. Keays (1976), Additional estimates of continental
655 surface Precambrian shield composition in Canada, *Geochim. Cosmochim. Acta*, *40*,
656 73-83.

657 Shaw, D. M., G. A. Reilly, J. R. Muysson, G. E. Pattenden, and F. E. Campbell (1967),
658 An estimate of the chemical composition of the Canadian Precambrian shield,
659 *Can. J. Earth Sci.*, *4*, 829-853.

660 Smith, J., D. Vance, R. A. Kemp, C. Archer, P. Toms, M. King, and M. Zárate (2003),
661 Isotopic constraints on the source of Argentinian loess – with implications for
662 atmospheric circulation and the provenance of Antarctic dust during recent
663 glacial maxima, *Earth Planet. Sci. Lett.*, *212*(1–2), 181-196.

664 Sun, J. (2002), Provenance of loess material and formation of loess deposits on
665 the Chinese Loess Plateau, *Earth Planet. Sci. Lett.*, *203*(3–4), 845-859.

666 Taylor, S. R., and S. M. McLennan (1981), The composition and evolution of the
667 continental crust: rare earth element evidence from sedimentary rocks, *Phil.*
668 *Trans. R. Soc. Lond., A* *301*, 381-399.

669 Taylor, S. R., and S. M. McLennan (1985), *The Continental Crust: Its Composition*
670 *and Evolution*, 312 pp., Blackwell Scientific Publ., Oxford.

671 Taylor, S. R., and S. M. McLennan (1995), The geochemical evolution of the
672 continental crust, *Rev. Geophys.*, *33*(2), 241-265.

673 Taylor, S. R., S. M. McLennan, and M. T. McCulloch (1983), Geochemistry of loess,
674 continental crustal composition and crustal model ages, *Geochim. Cosmochim.*
675 *Acta*, *47*, 1897-1905.

676 Újvári, G., A. Varga, F. C. Ramos, J. Kovács, T. Németh, and T. Stevens (2012),
677 Evaluating the use of clay mineralogy, Sr-Nd isotopes and zircon U-Pb ages in
678 tracking dust provenance: An example from loess of the Carpathian Basin, *Chem.*
679 *Geol.*, *304–305*(0), 83-96.

680 van de Fliedert, T., S. L. Goldstein, S. R. Hemming, M. Roy, M. Frank, and A. N.
681 Halliday (2007), Global neodymium-hafnium isotope systematics -- revisited,
682 *Earth Planet. Sci. Lett.*, *259*(3-4), 432.

683 Vervoort, J. D., and P. J. Patchett (1996), Behavior of hafnium and neodymium
684 isotopes in the crust: Constraints from Precambrian crustally derived granites,
685 *Geochim. Cosmochim. Acta*, *60*(19), 3717-3733.

686 Vervoort, J. D., and J. Blichert-Toft (1999), Evolution of the depleted mantle: Hf
687 isotope evidence from juvenile rocks through time, *Geochim. Cosmochim. Acta*,
688 *63*(3/4), 533-556.

689 Vervoort, J. D., T. Plank, and J. Prytulak (2011), The Hf-Nd isotopic composition of
690 marine sediments, *Geochim. Cosmochim. Acta*, *75*(20), 5903-5926.

691 Vervoort, J. D., P. J. Patchett, J. Blichert-Toft, and F. Albarède (1999),
692 Relationships between Lu-Hf and Sm-Nd isotopic systems in the global
693 sedimentary system, *Earth Planet. Sci. Lett.*, *168*, 79-99.
694 Vervoort, J. D., P. J. Patchett, F. Albarède, J. Blichert-toft, R. Rudnick, and H.
695 Downes (2000), Hf-Nd isotopic evolution of the lower crust, *Earth Planet. Sci.*
696 *Lett.*, *181*, 115-129.
697 Vlastelic, I., M. Carpentier, and E. Lewin (2005), Miocene climate change
698 recorded in the chemical and isotopic (Pb, Nd, Hf) signature of Southern Ocean
699 sediments, *Geochem. Geophys. Geosyst.*, *6*, Q03003.
700 Wang, C. Y., I. H. Campbell, C. M. Allen, I. S. Williams, and S. M. Eggins (2009), Rate
701 of growth of the preserved North American continental crust: Evidence from Hf
702 and O isotopes in Mississippi detrital zircons, *Geochim. Cosmochim. Acta*, *73*(3),
703 712-728.
704 Wedepohl, K. H. (1995), The composition of the continental crust, *Geochimica*
705 *Cosmochimica Acta*, *59*, 1217-1232.
706 White, W. M., and B. Dupré (1986), Sediment subduction and magma genesis in
707 the lesser Antilles: Isotopic and trace element constraints, *J. Geophys. Res.*, *91*,
708 5927-5941.
709 Woodhead, J. D., J. M. Hergt, J. P. Davidson, and S. M. Eggins (2001), Hafnium
710 isotope evidence for 'conservative' element mobility during subduction zone
711 processes, *Earth Planet. Sci. Lett.*, *192*, 331-346.
712 Yang, S., F. Ding, and Z. Ding (2006), Pleistocene chemical weathering history of
713 Asian arid and semi-arid regions recorded in loess deposits of China and
714 Tajikistan, *Geochim. Cosmochim. Acta*, *70*(7), 1695-1709.
715 Yao, J., L. Shu, and M. Santosh (2011), Detrital zircon U-Pb geochronology, Hf-
716 isotopes and geochemistry—New clues for the Precambrian crustal evolution of
717 Cathaysia Block, South China, *Gondwana Research*, *20*(2-3), 553-567.
718 Yoshida, M. (2012), Dynamic role of the rheological contrast between cratonic
719 and oceanic lithospheres in the longevity of cratonic lithosphere: A three-
720 dimensional numerical study, *Tectonophysics*, *532-535*(0), 156-166.
721 Zartman, R. E., and B. R. Doe (1981), Plumbotectonics - the model, *Tectonophys.*,
722 *75*, 135-162.

723

724

725 **Table captions:**

726

727 **Table 1:** Nd and Hf isotopic results for all loess samples.

728 Footnotes: All ϵ_{Nd} and ϵ_{Hf} values were calculated using the BSE value suggested
729 by Bouvier et al. [2008]. Dup stands for complete duplicate analyses. The
730 $^{147}Sm/^{144}Nd$ and $^{176}Lu/^{177}Hf$ are calculated using the Sm, Nd, Lu and Hf
731 concentration data listed in the Supplementary table.

732

733 **Table 2:** Compilation of the parent-daughter ratios and Nd and Hf isotopic
734 compositions of various reservoirs.

735 Footnotes: Numbers in italics correspond to ratios recalculated using published
736 concentrations. *: values used to calculate T_{DM} . Data sources: Allègre and
737 Rousseau [1984], Bouvier et al. [2008], Chauvel et al. [2008], Condie [1993],
738 Condie et al. [2011], Dhuime et al. [2011], Gale et al. [2013], Gao et al. [1998],
739 Goldstein et al. [1984], Goodge and Vervoort [2006], Griffin et al. [2002],
740 Hawkesworth et al. [2010], Jahn and Condie [1995], McCulloch and Wasserburg
741 [1978], Rudnick and Gao [2003], Salters and Stracke [2004], Shaw et al. [1967;
742 1976], Taylor and McLennan [1985] and Wedepohl [1995].

743

744 **Supplementary table:** Trace element concentrations measured on all loess
745 samples as well as values published by Gallet et al. [1996] for the Luochuan loess.

746 **Supplementary figure:** Comparison between the new trace element data and
747 the data published previously by Jahn et al. [2001].

748

749 **Figure captions:**

750 **Figure 1:** Map of the world showing the location of loess deposits. The precise
751 locations of Western European, Chinese, Argentinian and Tajikistan loess
752 samples were provided by Gallet et al. [1996; 1998], Jahn et al. [2001] and Ding
753 et al. [2002]. The Sahara samples blown over Southern Europe were collected
754 close to Grenoble and at 2900 m altitude in the Alps. Latitudes and longitudes are
755 given in the Supplementary Table.

756

757 **Figure 2:** Trace element patterns of the loess samples. All concentrations are
758 normalized to the upper continental crust average of Rudnick and Gao [2003]. a)
759 Western European loess, b) all Chinese loess including data published by Gallet
760 et al. [1996], c) Tajikistan loess and d) Argentinian loess and Sahara dust.

761

762 **Figure 3:** Nd and Hf isotopic compositions of loess samples. ϵ_{Nd} and ϵ_{Hf} were
763 calculated using the BSE value of Bouvier et al. [2008]. The terrestrial array
764 corresponds to $\epsilon_{Hf} = 1.55 \cdot \epsilon_{Nd} + 1.21$ as recently compiled by Vervoort et al. [2011].
765 Data for MORB and OIB were compiled using the PetDB and Georoc databases
766 and also include some unpublished values of Chauvel. Oceanic sediments plotted
767 here were published in the literature [*White and Dupré, 1986; BenOthman et al.,*
768 *1989; McLennan et al., 1990; Godfrey et al., 1997; Albarède et al., 1998; Pearce et*
769 *al., 1999; Vervoort et al., 1999; David et al., 2001; Woodhead et al., 2001; Vlastelic*
770 *et al., 2005; Prytulak et al., 2006; van de Fliedrt et al., 2007; Carpentier et al.,*
771 *2008; Bayon et al., 2009; Carpentier et al., 2009; Chauvel et al., 2009; Vervoort et*
772 *al., 2011*]. Data source for continental crust were published by Vervoort and
773 Patchett [1996] and by Vervoort et al. [1999; 2000]. The inset shows how our
774 estimated upper continental crust composition (red star) relates to the range of
775 known isotopic values in the Earth.

776

777 **Figure 4:** Nd/Hf versus $\Delta\epsilon_{Hf}$ for all the analyzed loess samples. The inset shows
778 schematically how the $\Delta\epsilon_{Hf}$ values are calculated for each sample. The terrestrial
779 array used to calculate $\Delta\epsilon_{Hf}$ values corresponds to $\epsilon_{Hf} = 1.55 \cdot \epsilon_{Nd} + 1.21$ as recently
780 reevaluated by Vervoort et al. [2011]. Shown by arrows along the horizontal axis
781 are various estimates for Upper Continental Crust: Taylor and McLennan [1985],
782 Shaw et al. [1967; 1976], Rudnick and Gao [2003], Condie [1993] and Gao et al.
783 [1998].

784

785

786 **Figure 5:** T_{DM} (Nd) versus T_{DM} (Hf) for all loess samples.

787 The T_{DM} (Nd) are calculated using the $^{147}\text{Sm}/^{144}\text{Nd}$ ratio measured for each
788 sample. They are well constrained with an error smaller than the horizontal bars.
789 The T_{DM} (Hf) ages are calculated using a single stage Lu/Hf evolution for the
790 samples coming from China, Tajikistan, Argentina and Sahara, and using a two
791 stages evolution for the samples from Western Europe. For the latter, we
792 assumed that the average crystallization age of the excess zircons was 0.9 Ga, an

793 age consistent with the Archean to Proterozoic materials that have been
794 repeatedly reworked during the Cadomian and Hercynian orogenies [*Peucat et*
795 *al.*, 1988]. For all samples, the vertical bar corresponds to the range of ages
796 obtained with a $^{176}\text{Lu}/^{177}\text{Hf}$ ratio going from 0.0057 (the youngest ages) to
797 0.0200 (the oldest ages). The inset shows how the two-stages calculation
798 operates. A “zircon stage” is calculated between present-day and a crystallization
799 age T_{cryst} of 900 Ma, and using a $^{176}\text{Lu}/^{177}\text{Hf}$ ratio of 0.0001. Prior to T_{cryst} , the
800 evolution follows the same range of UCC $^{176}\text{Lu}/^{177}\text{Hf}$ ratios as for all other
801 samples. The inset also highlights how single stage crustal model ages become
802 significantly too old if the zircons did not crystallize recently.

803

804 **Figure 6:** Measured $^{147}\text{Sm}/^{144}\text{Nd}$ versus calculated $^{176}\text{Lu}/^{177}\text{Hf}$ for all loess
805 samples.

806 As in Figure 5, a single stage history is assumed for the Argentinian, Chinese,
807 Tajikistan and Sahara samples and a two-stages history for the Western
808 European samples. The grey field corresponds to the range of published values
809 for the Lu/Hf ratio of upper continental crust [*Shaw et al.*, 1967; *Taylor and*
810 *McLennan*, 1985; *Condie*, 1993; *Gao et al.*, 1998; *Griffin et al.*, 2002; *Rudnick and*
811 *Gao*, 2003; *Goodge and Vervoort*, 2006; *Hawkesworth et al.*, 2010; *Condie et al.*,
812 2011]. The two red lines show our estimated averages and the orange fields
813 correspond to the calculated error at 1σ .

814

Highlights

- First estimate of the average Nd-Hf isotopic composition of upper continental crust
- The average ($\epsilon_{\text{Nd}} = -10.3 \pm 1.2$ and $\epsilon_{\text{Hf}} = -13.2 \pm 2$) falls on the terrestrial array
- The average Nd model age of upper continental crust is 1.82 ± 0.07 Ga
- The upper continental crust $^{176}\text{Lu}/^{177}\text{Hf}$ ratio is 0.0125 ± 0.0018

Figure 1

[Click here to download Figure: Figure 1 revised.pdf](#)

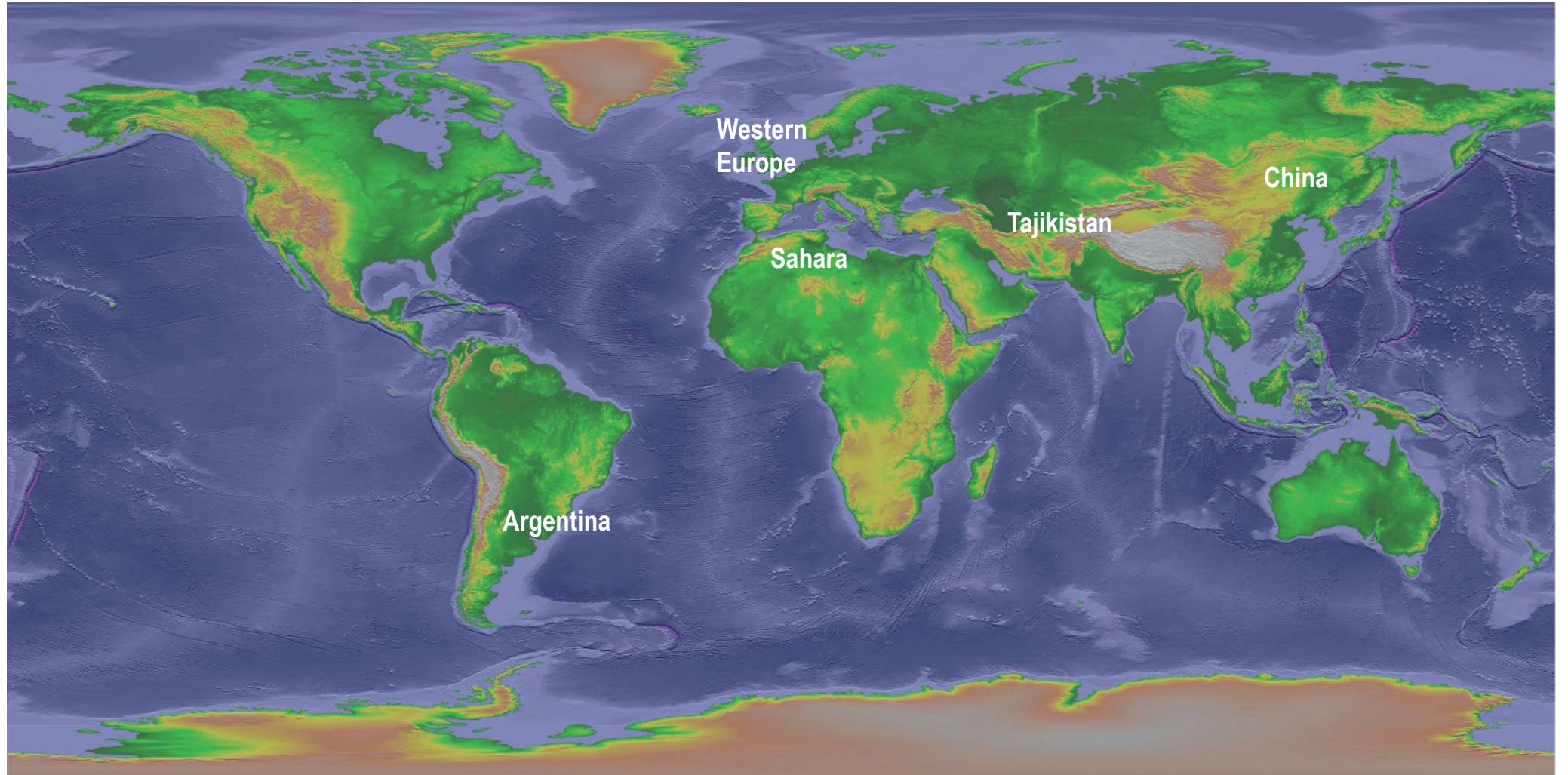


Figure 1

Figure 2

[Click here to download Figure: Figure 2 revised.pdf](#)

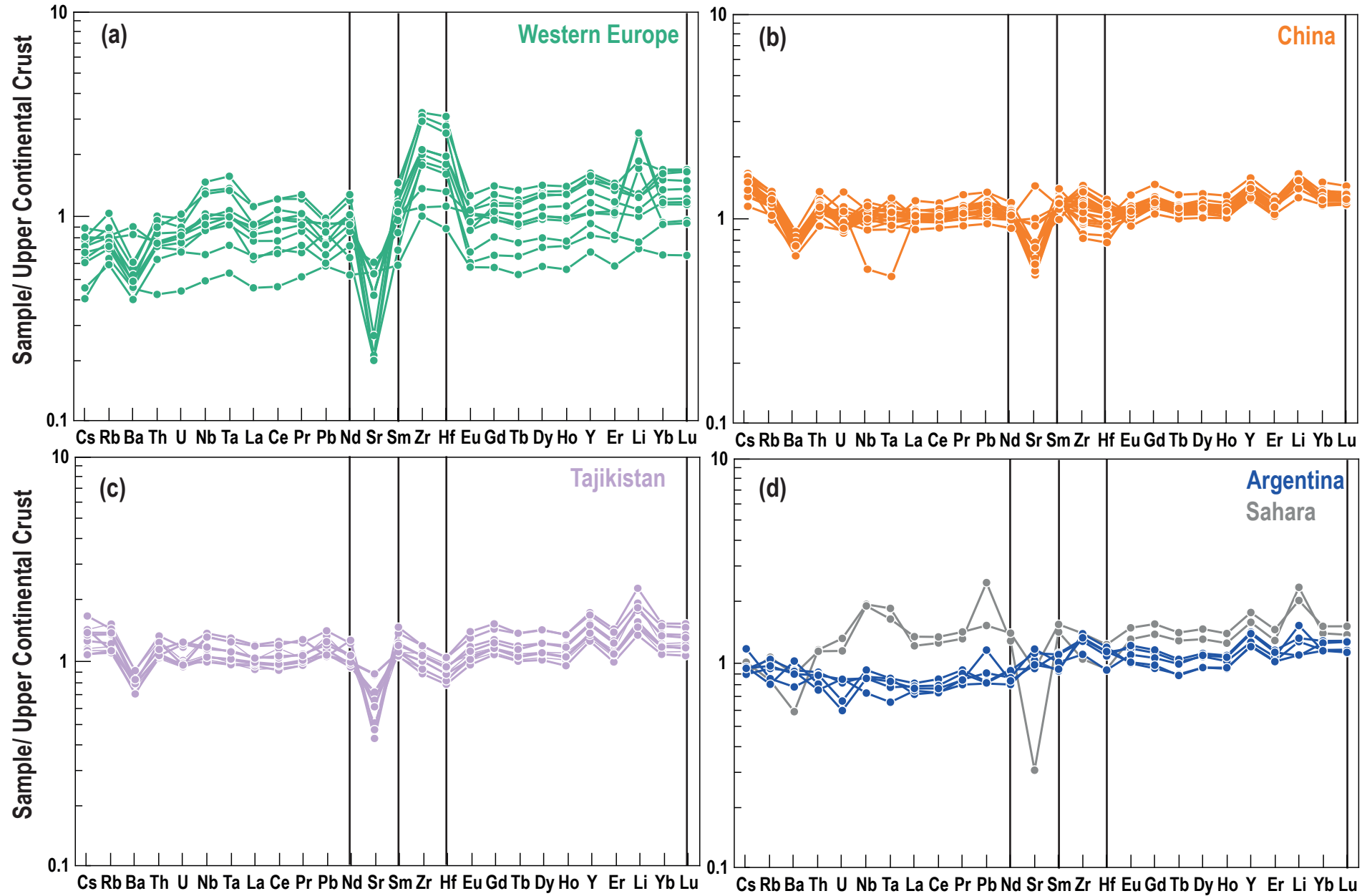


Figure 2

Figure 3

[Click here to download Figure: Figure 3 revised.pdf](#)

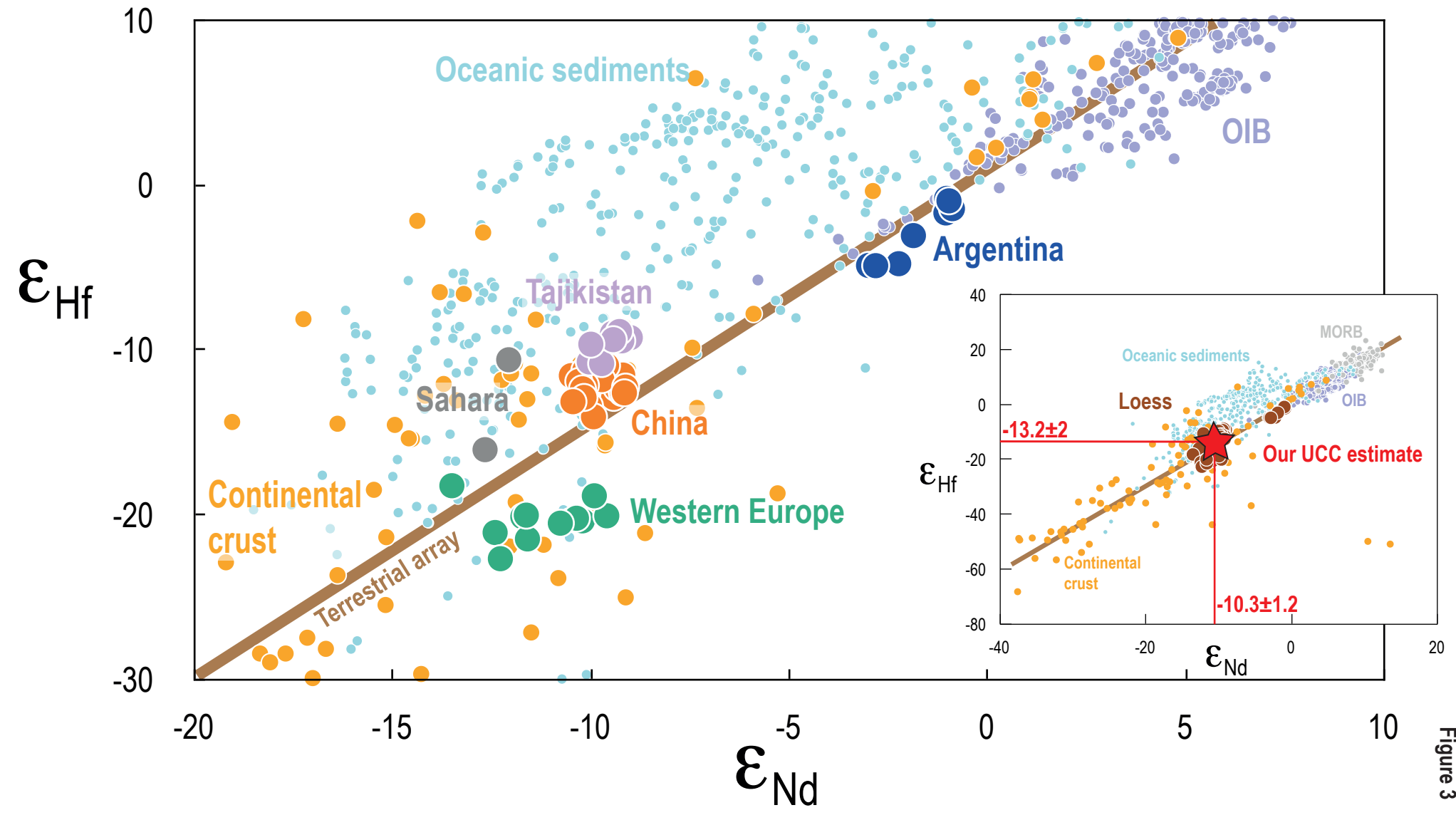


Figure 3

Figure 4

[Click here to download Figure: Figure 4 revised.pdf](#)

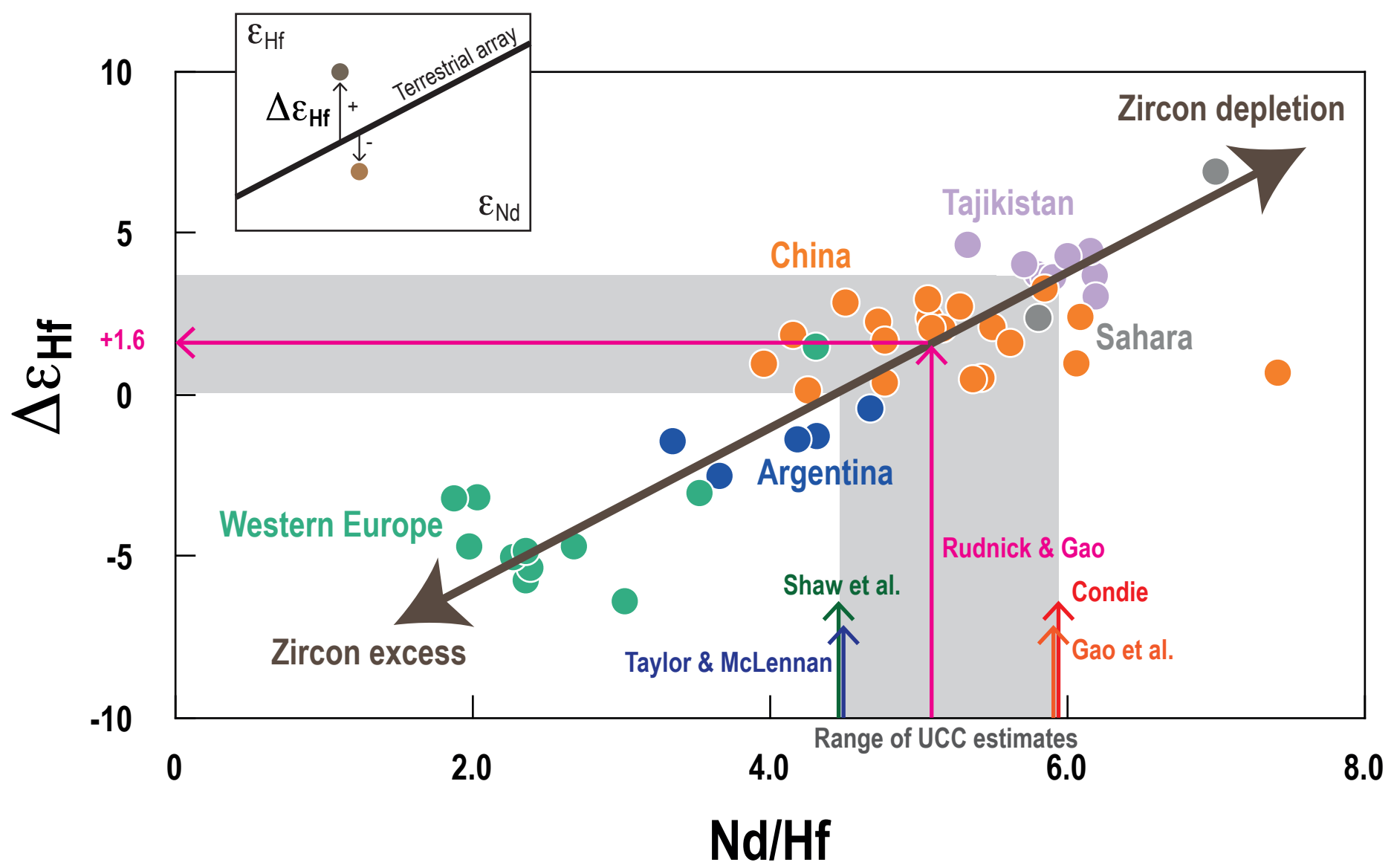


Figure 4

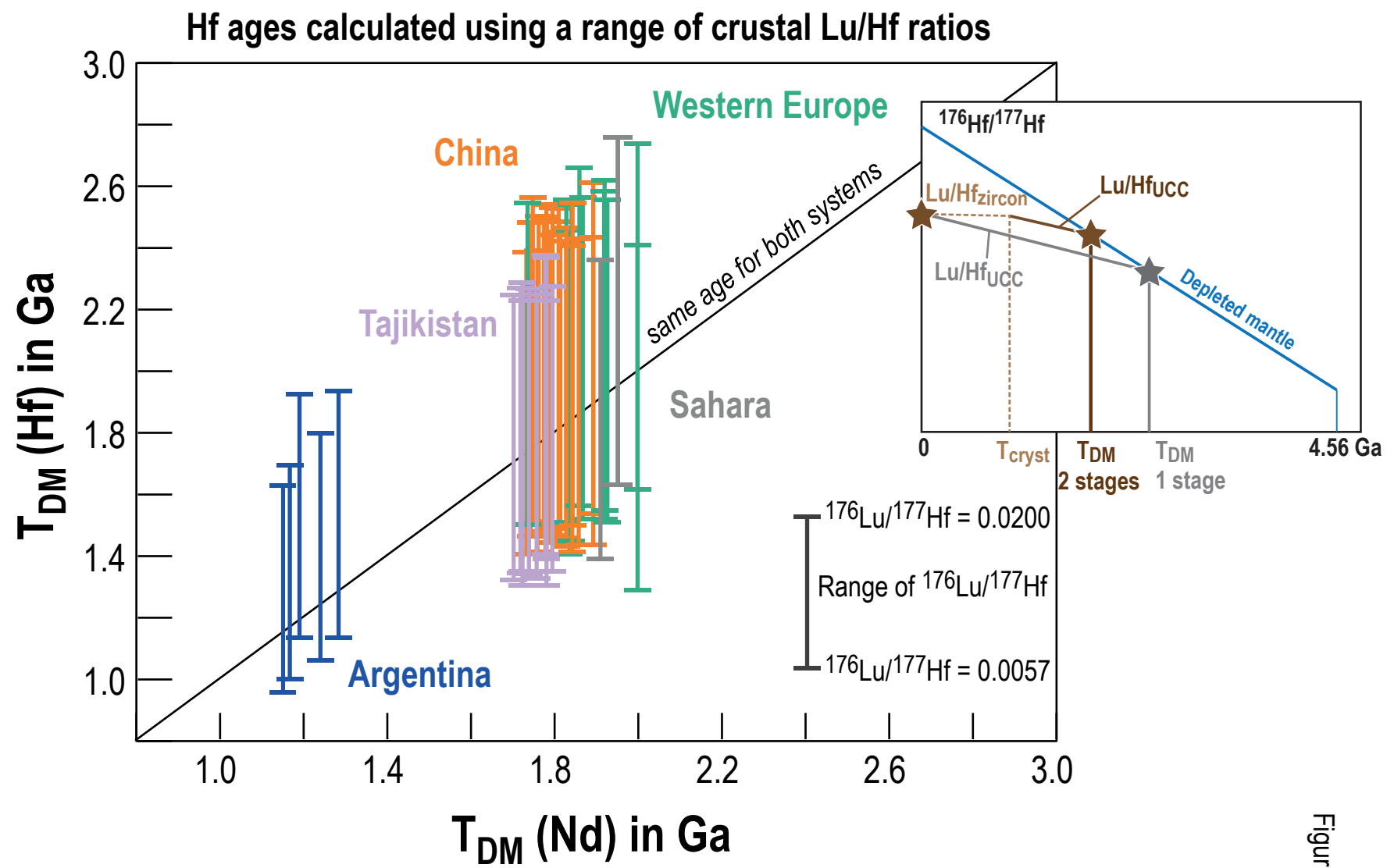


Figure 5

Figure 6

[Click here to download Figure: figure 6 revised.pdf](#)

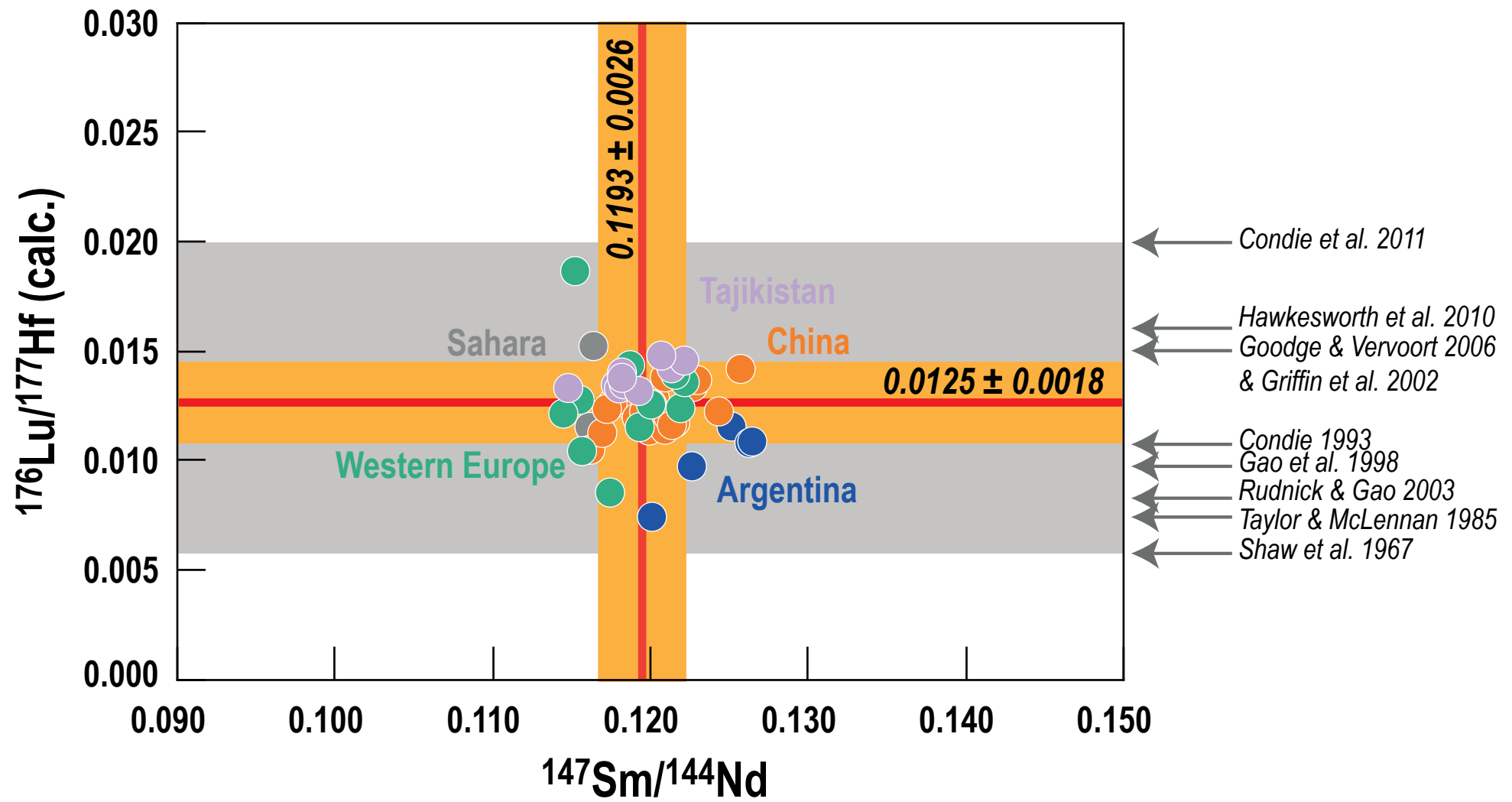


Figure 6

Table 1: Nd and Hf isotopic compositions of the loess samples

Sample	Location	$^{143}\text{Nd}/^{144}\text{Nd}$ d	2s	ϵ_{Nd}	$^{147}\text{Sm}/^{144}\text{Nd}$ d	$^{176}\text{Hf}/^{177}\text{Hf}$ f	2s	ϵ_{Hf}	$^{176}\text{Lu}/^{177}\text{Hf}$
Western Europe									
HOT1 whole rock	St Brieuc, France	0.512106	0.000009	-10.2	0.1219	0.282209	0.000008	-20.4	0.00574
HOT1 < 160 mm	St Brieuc, France	0.512098	0.000010	-10.4	0.1193	0.282213	0.000007	-20.2	0.00541
PR RT (whole rock)	Port Racine, Normandy, France	0.512078	0.000009	-10.8	0.1222	0.282205	0.000013	-20.5	0.00477
FOUG 3a<160 mm	Fougères, France	0.512029	0.000006	-11.7	0.1187	0.282216	0.000006	-20.1	0.00537
SAB 1a <160 mm	Sables d'or, France	0.512138	0.000009	-9.6	0.1174	0.282218	0.000015	-20.1	0.00613
NS 6 < 160 mm	Nantois, France	0.512121	0.000006	-9.9	0.1216	0.282252	0.000012	-18.9	0.00634
LO94	Spitsbergen (Svalbard)	0.511937	0.000010	-13.5	0.1152	0.282269	0.000010	-18.2	0.00905
P2E1	Spitsbergen (Svalbard)	0.511993	0.000009	-12.4	0.1155	0.282189	0.000013	-21.1	0.00717
K14	Kesselt, Belgium	0.512000	0.000011	-12.3	0.1200	0.282144	0.000006	-22.7	0.00509
R 11	Rocourt, Belgium	0.512035	0.000009	-11.6	0.1156	0.282178	0.000010	-21.5	0.00451
SCIL	Scilly Island, England	0.512034	0.000008	-11.6	0.1145	0.282219	0.000018	-20.0	0.00464
China									
JX-4	Jixian	0.512110	0.000008	-10.1	0.1203	0.282442	0.000011	-12.1	0.00987
JX-6	Jixian	0.512101	0.000015	-10.3	0.1188	0.282448	0.000013	-11.9	0.00855
JX-10	Jixian	0.512115	0.000009	-10.0	0.1162	0.282406	0.000011	-13.4	0.00843
JX-2	Jixian	0.512106	0.000007	-10.2	0.1189	0.282435	0.000008	-12.4	0.00976
XF-10	Xifeng	0.512124	0.000009	-9.9	0.1176	0.282470	0.000009	-11.1	0.01011
XF-6	Xifeng	0.512131	0.000011	-9.7	0.1201	0.282451	0.000013	-11.8	0.01010
XF-2	Xifeng	0.512162	0.000008	-9.1	0.1199	0.282438	0.000013	-12.3	0.01344
XF-4	Xifeng	0.512160	0.000010	-9.2	0.1209	0.282429	0.000014	-12.6	0.00948
XF-4 dup	Xifeng					0.282443	0.000008	-12.1	
XN-2	Xining	0.512102	0.000009	-10.3	0.1169	0.282414	0.000009	-13.1	0.01078
XN-4	Xining	0.512120	0.000011	-9.9	0.1243	0.282388	0.000010	-14.1	0.00880
XN-10	Xining	0.512108	0.000008	-10.2	0.1191	0.282421	0.000010	-12.9	0.00911
XN-6	Xining	0.512094	0.000008	-10.5	0.1196	0.282413	0.000008	-13.1	0.00835
L3	Luochuan	0.512146	0.000010	-9.4	0.1216	0.282421	0.000007	-12.9	0.01110
L4	Luochuan	0.512138	0.000010	-9.6	0.1257	0.282457	0.000014	-11.6	0.01082
L5	Luochuan	0.512150	0.000012	-9.4	0.1211	0.282437	0.000008	-12.3	0.01227
L6	Luochuan	0.512158	0.000009	-9.2	0.1213	0.282429	0.000005	-12.6	0.01114
L7	Luochuan	0.512140	0.000009	-9.6	0.1227	0.282460	0.000007	-11.5	0.01145
L7 dup	Luochuan	0.512158	0.000009	-9.2		0.282459	0.000009	-11.5	
L9	Luochuan	0.512137	0.000009	-9.6	0.1172	0.282475	0.000006	-11.0	0.01023
L1	Luochuan	0.512125	0.000010	-9.9	0.1229	0.282456	0.000014	-11.6	0.01194
L2	Luochuan	0.512109	0.000012	-10.2	0.1209	0.282467	0.000010	-11.2	0.01243
Argentina									
12-14	Argentina	0.512515	0.000009	-2.2	0.1201	0.282650	0.000005	-4.8	0.00821
24-26	Argentina	0.512577	0.000009	-1.0	0.1251	0.282762	0.000007	-0.8	0.01140
32RT	Argentina	0.512576	0.000008	-1.1	0.1263	0.282737	0.000006	-1.7	0.00984
32RT dup	Argentina	0.512580	0.000008	-1.0		0.282758	0.000006	-1.0	
40RT	Argentina	0.512534	0.000007	-1.9	0.1264	0.282698	0.000004	-3.1	0.00846
LUJA	Argentina	0.512476	0.000006	-3.0	0.1226	0.282647	0.000005	-4.9	0.00807
Sahara									
Sahara dust collected in Meylan	Meylan, France	0.511980	0.000007	-12.7	0.1161	0.282331	0.000008	-16.1	0.01020
Sahara dust collected at 2900m altitude	Alpes, France	0.512011	0.000007	-12.1	0.1164	0.282485	0.000005	-10.6	0.01220
Tajikistan									
TJK2772	Chashmanigar, Tajikistan	0.512163	0.000007	-9.1	0.1178	0.282526	0.000006	-9.2	0.01152
TJK2773	Chashmanigar, Tajikistan	0.512168	0.000011	-9.0	0.1213	0.282523	0.000005	-9.3	0.01206
TJK2930	Chashmanigar, Tajikistan	0.512115	0.000006	-10.0	0.1180	0.282482	0.000006	-10.7	0.01117
TJK3012	Chashmanigar, Tajikistan	0.512154	0.000006	-9.3	0.1221	0.282517	0.000004	-9.5	0.01163
TJK3070	Chashmanigar, Tajikistan	0.512157	0.000007	-9.2	0.1183	0.282518	0.000007	-9.5	0.01145
TJK3148	Chashmanigar, Tajikistan	0.512145	0.000006	-9.5	0.1207	0.282530	0.000006	-9.0	0.01189
TJK3179	Chashmanigar, Tajikistan	0.512154	0.000006	-9.3	0.1182	0.282534	0.000007	-8.9	0.01221
TJK3198	Chashmanigar, Tajikistan	0.512131	0.000008	-9.7	0.1192	0.282479	0.000006	-10.8	0.01146
TJK2814	Chashmanigar, Tajikistan	0.512146	0.000007	-9.4	0.1182	0.282520	0.000006	-9.4	0.01141
TJK3165	Chashmanigar, Tajikistan	0.512117	0.000009	-10.0	0.1148	0.282512	0.000007	-9.7	0.01056

Table2: Compilation of the parent-daughter ratios and Nd and Hf isotopic compositions of various reservoirs

Reservoir	Source	$^{143}\text{Nd}/^{144}\text{Nd}$	ϵ_{Nd}	Sm (ppm)	Nd (ppm)	$^{147}\text{Sm}/^{144}\text{Nd}$	$^{176}\text{Hf}/^{177}\text{Hf}$	ϵ_{Hf}	Lu (ppm)	Hf (ppm)	$^{176}\text{Lu}/^{177}\text{Hf}$
Bulk Silicate Earth	Bouvier et al. 2008	0.512630	-			0.1960	0.282785	-			0.0336
Most depleted MORB*	Chauvel et al. 2008	0.513270	12.48			0.2172	0.283381	21.08			0.0403
Depleted mantle	Salters and Stracke 2004			0.27	0.713	0.2289			0.063	0.199	0.0449
Average MORB	Chauvel et al. 2008	0.513072	8.62			0.2106	0.283208	14.96			0.0384
"	Gale et al. 2013	0.513074	8.66			0.2107	0.283000	7.6			0.0360
"	Gale et al. and Hf on terrestrial array	0.513074	8.66			0.2107	0.283199	14.63			0.0383
Source of new crust	Thiery et al. 2011 and Nd on terrestrial array	0.513027	7.74				0.283158	13.2			
Upper Continental crust											
	Rudnick and Gao TOG 2003			4.7	27	0.1052			0.31	5.3	0.0083
	Taylor and McLennan 1985			4.5	26	0.1046			0.32	5.8	0.0078
	Gao et al. 1998			5.09	30.4	0.1012			0.35	5.12	0.0097
	Shaw et al. 1967&1976			4.61	25.9	0.1076			0.233	5.8	0.0057
	Condie 1993			5.09	30.4	0.1012			0.32	4.3	0.0106
	Wedepohl 1995			4.7	25.9	0.1097			0.27	5.8	0.0066
	McCulloch and Wasserburg, 1978					0.1150					
	Goldstein et al. 1984					0.1150					
	Allègre and Rousseau 1984					0.1120					
	Jahn and Condie 1995					0.1180					
	Goodge and Vervoort 2006										0.0150
	Griffin et al. 2002										0.0150
	Hawkesworth et al. 2010										0.0159
	Condie et al. 2011										0.0200
Our estimate for Upper Continental Crust		0.512101	-10.3			0.1193	0.282412	-13.2			0.0125
uncertainty at one sigma		±0.000060	±1.2			±0.0026	±0.000060	±2			±0.0018

Supplementary table

[Click here to download Supplementary material for on-line publication only: supplementary file revised.xlsx](#)

Supplementary figure

[Click here to download Supplementary material for on-line publication only: supplementary figure.pdf](#)